BULETINUL INSTITUTULUI POLITEHNIC DIN IAŞI
Publicat de
Universitatea Tehnică „Gheorghe Asachi” din Iaşi
Volumul 63 (67), Numărul 1, 2017
Secţia
CONSTRUCŢII DE MAŞINI

DETECTION OF 2D CROSS SECTION PROFILE OF ROTATING OBJECTS USING A 1D OPTICAL LASER MEASUREMENT SYSTEM

BY

MIHĂIȚĂ HORODINCĂ*

"Gheorghe Asachi" Technical University of Iaşi,
Faculty of Machine Manufacturing and Industrial Management

Received: January 16, 2017
Accepted for publication: May 15, 2017

Abstract. The paper presents some research results related with a study on computer aided 2D cross section profile experimentally detection on rotating objects, particularly a four flute end mill used as cutting tool. A 1D laser optical relative displacement measurement system placed near the tool is used as sensor. The signal delivered by sensor is correlated with tool rotational motion features in order to produce the 2D shape of the cross section profile. There are enough elements of similarity with the real profile in order to have confidence in the quality of this detection. Thus the shape, the size and the integrity of cutting tool can be easy verified directly on the machine tool in order to increase the safety of exploitation (to prevent the work with a wrong or a damaged tool).

Keywords: cross section; profile; detection; optical sensor; signal processing.

1. Introduction

Many usual computer-assisted manufacturing systems in mechanics (*e.g.* machine tools) use the rotating interaction between parts (*e.g.* a cutting tool and a workpiece during milling, turning, drilling or grinding processes). An

*Corresponding author; *e-mail*: horodinca@tuiasi.ro

important item in the exploitation of these manufacturing systems -related with the aims of this paper- is the automatic detection of 2D cross section profiles of rotating objects (usually the cutting tools and workpieces) completed on machine tools, using optical methods, at least for two important reasons:

– a quick control for size, shape and integrity of cutting tool before, in-process and at the end of cutting process;

– a quick control for shape and dimensions of the workpiece before, in-process and eventually at the end of cutting process;

Both objectives generally increase the safety of exploitation in order to prevent or avoid the damaging of workpiece or machine.

In the literature some important results on this topic are reported. Thus (Bi *et al.*, 2010) proposes a deep survey of actually optical methods and signal data processing techniques used in 3D vision systems in industrial environment (reverse engineering, part location and alignment, inspection, virtual assembly). Some other reported research results are focused on specific problems of manufacturing as follows:

– Several researchers (Fernández-Roblesa *et al.*, 2017; Szydłowski *et al.*, 2016; Loizou *et al*., 2016; Ghosh *et al.*, 2007) presents some results related with wear measurement on cutting tools;

– Some other researchers (Quinsat and Quinsat, 2017; Svalina *et al.*, 2017; Dhanasekar and Ramamoorthy, 2010) presents some results related with surface roughness measurement after cutting process.

– The papers (Mendikute and Zatarain, 2013; Zatarain *et al.*, 2012) present some results related with parts alignment during assembly process.

These 3D vision systems need a machine vision structure, a data acquisition system and data processing techniques. Having in mind the aims of this paper (and also the proposed experimental equipment), it seems to be difficult to extract quickly essential information related with online detection of tool or workpiece condition.

For this purpose, the laser optical vision systems are more appropriate. A recently deep review on this topic was done in (Kapłonek and Nadolny, 2015).

Thus (Xing *et al*., 2016) present some researches result on wheel-set size of rail vehicle online detection. The same system is used in laser forming by (Ding *et al*., 2016) for online measurement of deformation. Generally a 1D displacement laser optical sensor is used. The 2D or 3D images are obtained using supplementary movements of sensor or target object. Some calibration studies for surface profiling are necessary as (Abu-Nabah *et al*., 2016; Ding *et al*., 2016) indicates.

This paper intend to explore some new research resources available in the detection of the 2D external cross section profile on rotating objects directly on machine tools using a fixed non-contact laser-optical 1D relative displacement sensor. In order to prove the availability of this experimental

study, the researches were focussed essentially on detection of a four flute end mill cross 2D cross section profile.

2. Experimental Procedure

The essential of this procedure is briefly exposed in Fig. 1. Let O be the centre of rotation of the object (whose 2D cross section profile should be determined) and ω the angular speed (assumed to be constant) around this centre.

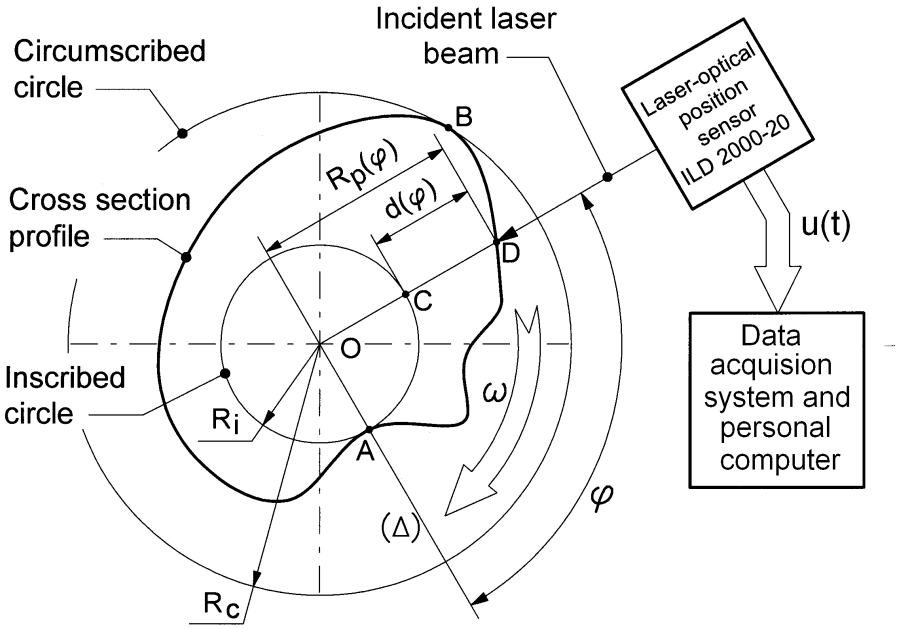

Fig. 1 − A conceptual presentation of the experimental setup.

Let B be the point of tangency between the circumscribed circle (with the centre placed in O) and cross section profile. Let A be the point of tangency between the inscribed circle (with the centre placed in O) and cross section profile. Let (Δ) be a line passing through the points O and A (this line also rotates with the angular speed ω). Let O, C and D be three points on a fixed line which is the same with the line of the incident laser beam delivered by a non contact laser-optical position sensor type ILD 2000-20 (http://www.img.ufl.edu/wiki/images/ILD_2000_Datasheet.pdf). This incident laser beam touch the surface of the rotating object in D, while C is the incidence point of the line OD with the inscribed circle. The point D is also a point of cross section profile. The points O and C are fixed on the line OD while usually the point D moves along the laser incident beam when the object rotates. The

diffused reflected laser beam from point D back to sensor (not depicted on Fig. 1) is used for optical triangulation in order to generate a voltage $u(t)$ which is directly proportional with the distance between sensor and the point D (if D is permanently placed in the measuring range of the sensor -20 mm- for a midrange distance to the sensor of 61 mm).

The evolution of voltage $u(t)$ can be correlated with the evolution of distance $d(\varphi)$ between the points C and D, see below in Eq. (1). Here $\varphi = \omega \cdot t$ is the angle of the line (Δ) related with the incident laser beam position and t is the symbol used to depict the time.

When $t = 0$, the points A, C and D coincide, the laser incident beam and the line (Δ) also coincides. At this moment the distance revealed by sensor is maximal the voltage $u(t)$ is also maximal ($u(t) = u_{max}$) and $d(\varphi)=0$ (here is the origin of measurement). When the point B coincide with D than the distance revealed by the sensor is minimal, the voltage $u(t)$ is also minimal ($u(t) = u_{min}$) and the distance $d(\varphi)$ takes the maximal value.

Let K be the constant of the laser sensor (the ratio between input displacement and output voltage). According with the sensor datasheet, the distance $d(\varphi)$ in the current position of the point D can be described as:

$$d(\varphi) = d(\omega \cdot t) = K \cdot [u_{max} - u(t)] \tag{1}$$

Let R_i be the radius of inscribed circle on Fig. 1 (assuming that this is a known value). The radius $R_p(\varphi)$ of the cross section profile in the current position of the point D (measured from point O) is described as follows:

$$R_p(\varphi) = R_i + d(\varphi) = R_i + K \cdot [u_{max} - u(t)] \tag{2}$$

In a 2D polar coordinate system with the pole in O and the line (Δ) as polar axis the cross section profile is completely described by the coordinates φ and $R_p(\varphi)$ of each point, with $\varphi = \omega \cdot t$ and $R_p(\varphi)$ given in Eq. (2).

In a 2D Cartesian coordinate system with the centre in O and the line (Δ) as x-axis (abscissa) the cross section profile is completely described by the coordinates x and y of each point, with $x = R_p(\varphi) \cdot \cos(\varphi)$ and $y = R_p(\varphi) \cdot \sin(\varphi)$.

In order to describe the 2D cross section profile is necessary to know the values for R_i, K and the evolution of $u(t)$ voltage (and u_{max} as well). The value of angular speed ω and the position of line (Δ) as origin for $d(\varphi)$ results usually from evolution of $u(t)$ voltage.

The voltage $u(t)$ is acquired in numerical format and processed - according with Eqs. (1) and (2)- on a personal computer through a data acquisition system based on a computer assisted numerical oscilloscope type PicoScope 4424 (https://www.picotech.com/download/datasheets/picoscope-4000-series-data-sheet.pdf).

The accuracy of profile description depends by the capability of sensor to generate a voltage $u(t)$ strictly related with the cross section profile. Some normal features of the surface where the profile is defined can generate a bad accuracy of the voltage (*e.g.* sharp edges, hidden parts of the profile related to incident laser beam, variation of surface reflectivity under the laser light, etc.). Some features of the electronic part of the sensor can also introduce some discrepancies in the mirroring of the voltage based on voltage evolution. Two features are especially critical: the relatively low values of resolution (1 μm) of measured distance and a low sampling rate (S = 10,000 s^{-1}). This last feature does not allow a high angular speed for the object involved in cross section profile detection. If the object turns with angular speed $\omega = 2 \cdot \pi \cdot f$ (f being the frequency of rotation), then the cross section profile is defined with S/f samples (or S/f points). In order to obtain the graphical description of the profile, these points are joined usually with line segments. A high accuracy of the profile means also a high number of samples (points) so a low frequency of rotation. However, we will consider here S as having an infinite value, hoping that a future sensing technique (with analog output voltage $u(t)$) will remove this limitation.

Despite these apparently serious inconveniences, the experiments prove that the procedures described in this paper produce trustworthy results.

3. Signal Processing Technique and Experimental Results

The above theoretical considerations were used to detect the cross section profile of a four flute end mill (16 mm diameter). Fig. 2 presents a general view of the experimental setup. Here are revealed the optical laser sensor (labelled with 1), the tool (labelled with 2) clamped in a three jaw chuck on a lathe and the point where the incident laser beam touch the tool (labelled with 3). All the experimental conditions imposed in Fig. 1 are fulfilled here.

Fig. 2 − A partial view on the experimental setup.

Fig. 3*a* presents a theoretical approach of a 2D cross section profile of this tool. Here are depicted the two relevant reasons for a bad accuracy of profile detection: the sharp edges (depicted as Se) and hidden areas (depicted as Ha). Fig. 3*b* shows how the profile should be described in the presence of hidden areas on the tool (a theoretical approach) assuming that the sensor describes correctly the sharp edges.

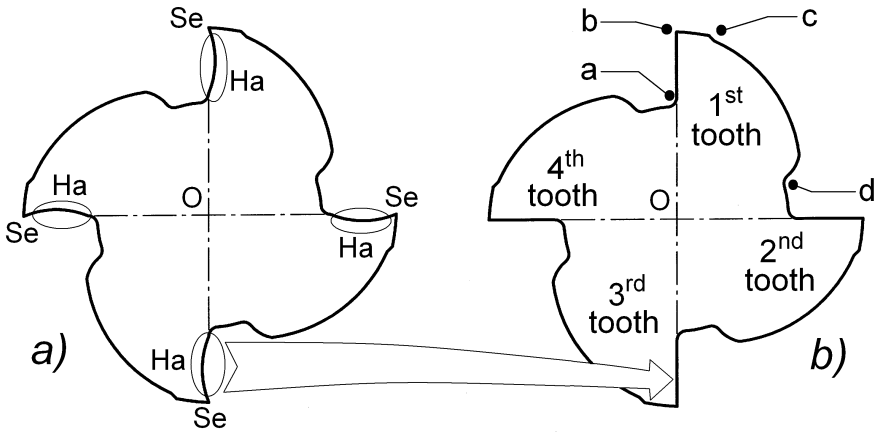

Fig. 3 – *a*) Theoretical shape of a 2D cross section profile for a four flute end mill; *b*) A theoretical approach of the profile described by sensor (the hidden areas are missing).

Fig. 4 presents the evolution of voltage $u(t)$ generated by optical laser sensor due to rotation of the four flute end mill in experimental condition depicted above.

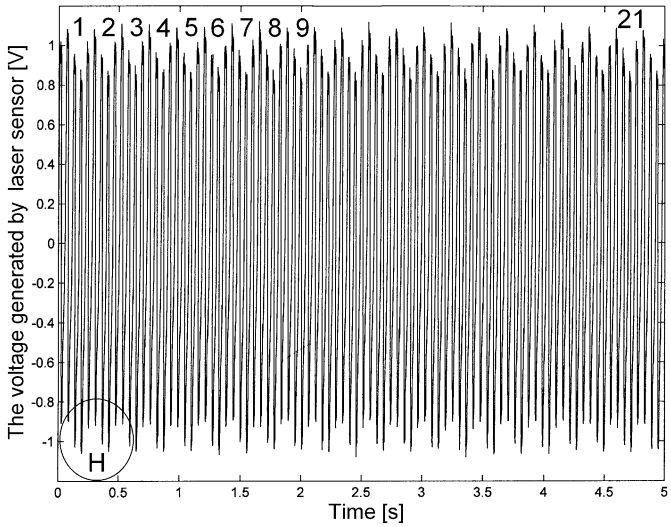

Fig. 4 – The evolution of the voltage $u(t)$ generated by optical laser sensor during the rotation of the four flute end mill.

As expected, this is a typical alternative voltage signal, due to the periodic variation of $R_p(\varphi)$ radius on cross section profile. A detail of this evolution (within zone H) is depicted in Fig. 5.

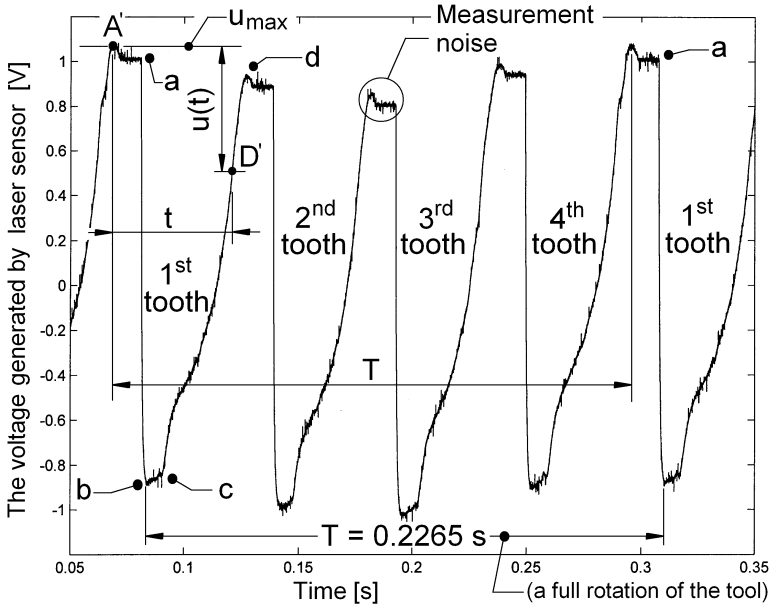

Fig. 5 – A detail of the evolution depicted in Fig. 4 (within zone H).

Each of four teeth on milling tool from Fig. 3*b* is described by a negative peak of voltage on Fig. 5. There is a good correspondence between Figs. 3*b* and 5 (see also the zones depicted with a, b, c and d on both figures). On this figure the value of rotational period -T = 0.2265 s, automatically measured during the computer aided signal processing- is useful for angular speed calculus ($\omega = 2 \cdot \pi / T$ = 27.740 rad/s) which corresponds to a rotational speed of 264.90 rpm.

There is a misalignment of the peaks of voltage (related to the teeth position) on Fig. 5 generated by the tool run-out, due to a faulty fastening of tool in the three jaw chuck, deliberately done in this experiment.

On Fig. 5 are also depicted the points A' and D', related with the consideration done on Fig. 1. The point A' on Fig. 5 correspond to A on Fig. 1. In A is the origin of angle φ (with φ = 0) which correspond to zero value for $d(\varphi)$ and also to the maximal value for the voltage (u_{max}) generated by sensor. This maximal voltage is retrieved in the point A' on Fig. 5. If in A is the origin for angle φ then in A' is the origin of time t. The current value of this angle (related to the point D on Fig. 1) is described by the delay t between the points A' and D' on Fig. 5 as it follows:

$$\varphi = \frac{t}{T} \cdot 2 \cdot \pi \tag{3}$$

The current value of the voltage $u(t)$ -involved in Eqs. (1) and (2)- generated by sensor, corresponds to the difference of ordinates of points A' and D' from Fig. 5. Assuming that the values of K and R_i from Eq. (2) are previously determined (K = 2.0751 mm/V and R_i = 4.25 mm) the value of current radius $R_p(\varphi)$ of the cross section profile can be easy calculated according to Eq. (2). Now the profile is completely determined in a 2D polar coordinate system -each point having the coordinates (φ, $R_p(\varphi)$- or in a 2D Cartesian coordinate system, each point having the coordinates $x = R_p(\varphi)\cdot\cos(\varphi)$ and $y = R_p(\varphi)\cdot\sin(\varphi)$.

As Fig. 5 indicates, there is a measurement noise on the signal delivered by optical laser sensor. There are two ways to strongly reduce the influence of this noise on the cross section profile. First way (which is not preferred here) is a numerical low pass filtering of the signal. The numerical filtering removes the noise but also change significantly the useful part of the signal and consequently the shape of the profile. The second way (used here) produces the voltage generated on a single theoretical rotation of the tool as an average of the values of voltage for several subsequent rotations (*e.g.* 21 rotations as marked on Fig. 4). The averaging increases also the accuracy of the profile detection.

This signal averaging is done using a numerical procedure as presented below. Let Δt be the sampling interval used to describe the discrete form of the voltage generated by sensor, generally written as $u(n\cdot\Delta t)$, with $t = n\cdot\Delta t$. Let m be the number of samples Δt which describes the rotational period as $T = m\cdot\Delta t$. Let p be the number of subsequent rotation of the tool. Let's suppose that m and p are integers. The current value of average voltage on a single rotation (generally written as $\bar{u}(k\cdot\Delta t)$, with k = 0 ÷ m-1) is described by:

$$\bar{u}(k\cdot\Delta t) = \frac{1}{p}\cdot\sum_{i=1}^{i=p} u(n\cdot\Delta t) \tag{4}$$

with:

$$n = k + (i-1)\cdot m \tag{5}$$

with the definition of time as $t = k\cdot\Delta t$ -from Eq. (4)- and period as $T = m\cdot\Delta t$ the polar angle φ from Eq. (3) becomes:

$$\varphi = \frac{k}{m}\cdot 2\cdot\pi = k\cdot\frac{2\cdot\pi}{m} = k\cdot\Delta\varphi \tag{6}$$

Here $\Delta\varphi = 2\cdot\pi/m$ is the polar angle increment.

The voltage $\bar{u}(k\cdot\Delta t)$ replaces the voltage $u(t)$ in Eqs. (1) and (2) in order to find out the average values of coordinates of points on the cross section profile in a polar system (φ and $\bar{R}_p(\varphi)$) or in a Cartesian system ($\bar{x}=\bar{R}_p(\varphi)\cdot\cos(\varphi)$ and $\bar{y}=\bar{R}_p(\varphi)\cdot\sin(\varphi)$).

If the ratio $m=T/\Delta t$ is not an integer (and it is big enough) then m need to be considered as the nearest integer of $T/\Delta t$.

Fig. 6 presents the evolution of $\bar{d}(t)$ -or $\bar{d}(\varphi)$ - distance in a Cartesian system of coordinates (t or φ on x-axis and $\bar{d}(\varphi)$ on y-axis), during a completely rotation of the tool, booth related with A" as origin of time and origin of polar angle respectively. Here A" is an image of the point A' from Fig. 5 and the point A from Fig. 1.

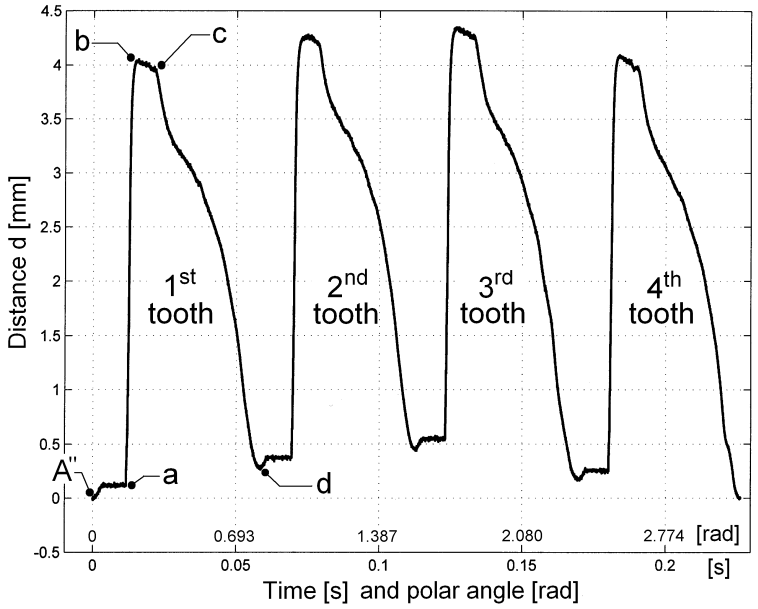

Fig. 6 – The evolution of $\bar{d}(t)$ -or $\bar{d}(\varphi)$ - distance in a 2D Cartesian coordinate system for a complete rotation of milling tool
(with T = 0.2265 s, m = 45300, p = 5, Δt = 5 μs, $\Delta\varphi$ = 138 μrad).

The letters a, b, c and d are used here (and also on Figs. 3*b*, 5, 7 and 9) in order to identify the essential parts of the first tooth, placed in the origin of a 2D Cartesian system coordinate system. The signal averaging here was done for a low value of p (p = 5) because during the experiment the rotational speed of the tool slightly decreases (and the period T slightly increases) so, for a high value of p the average profile will be distorted. A future approach will remove easy this inconvenience by an accurate measuring of period T for each rotation.

A representation of $\overline{d}(\varphi)$ evolution as a close trajectory in a 2D polar coordinate system (each point having the coordinates φ and $\overline{d}(\varphi)$) or in a 2D Cartesian coordinate system (each point having the coordinates $\overline{x} = \overline{d}(\varphi) \cdot \cos(\varphi)$ and $\overline{y} = \overline{d}(\varphi) \cdot \sin(\varphi)$) is given in Fig. 7. Of course this trajectory describes a particular form of experimental description of the 2D cross section profile of the four flute end mill (with φ and $\overline{R}_p(\varphi)$ the coordinates in a polar system or $\overline{x} = \overline{R}_p(\varphi) \cdot \cos(\varphi)$ and $\overline{y} = \overline{R}_p(\varphi) \cdot \sin(\varphi)$ the coordinates in a Cartesian system) assuming that $R_i = 0$.

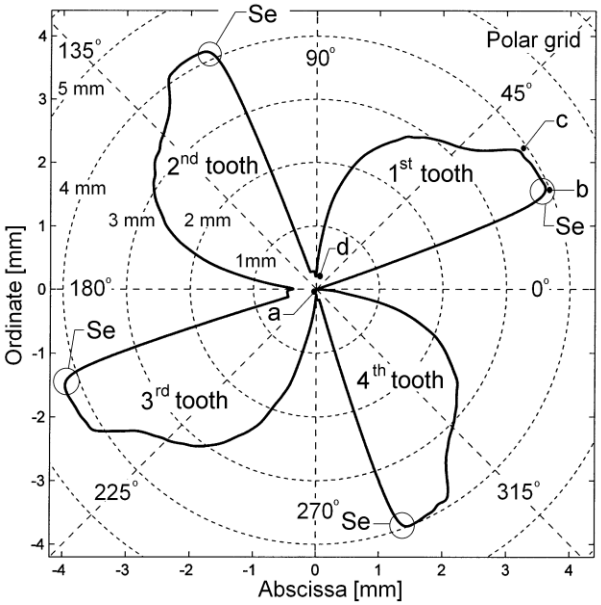

Fig. 7 – A particular form of experimental description for 2D cross section profile of the four flute end mill with $R_i = 0$ (slightly low pass numerical filtered).

This profile can be accepted as result of experimental investigations when the radius R_i of inscribed circle (Fig. 1) is unknown. It is sure that certain disadvantages already mentioned in Fig. 3*a* occur here: a bad accuracy of the sharp edges Se (shown here as having rounded shapes) and the impossibility to describe the hidden areas (Ha on Fig. 3*b*). This means firstly that the cutting edges wear cannot be easy detected by this procedure.

Many other features of the profile are available in the experimental automatic detection of tool damage such as: the milling tool run-out (see the profile related to the circle of 4 mm radius on polar grid), the shape, the symmetry and the integrity of the teeth (braking, cracking), built-up edges, etc.

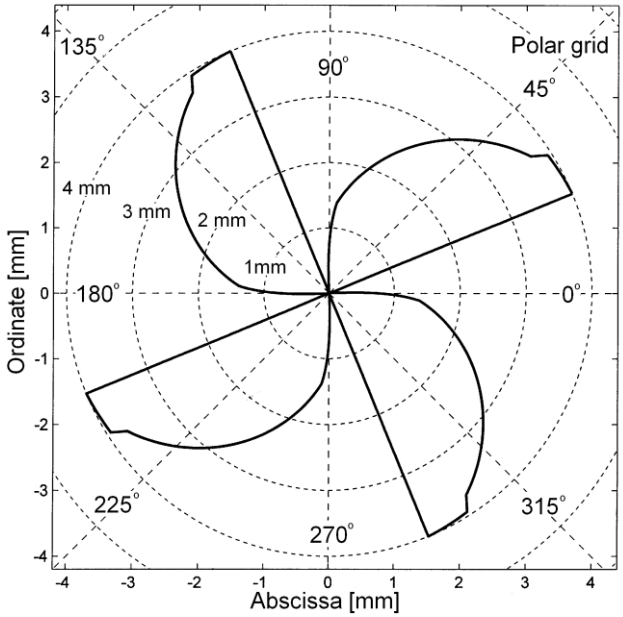

Fig. 8 – The shape depicted in Fig. 7 obtained by numerical simulation on a perfect tool.

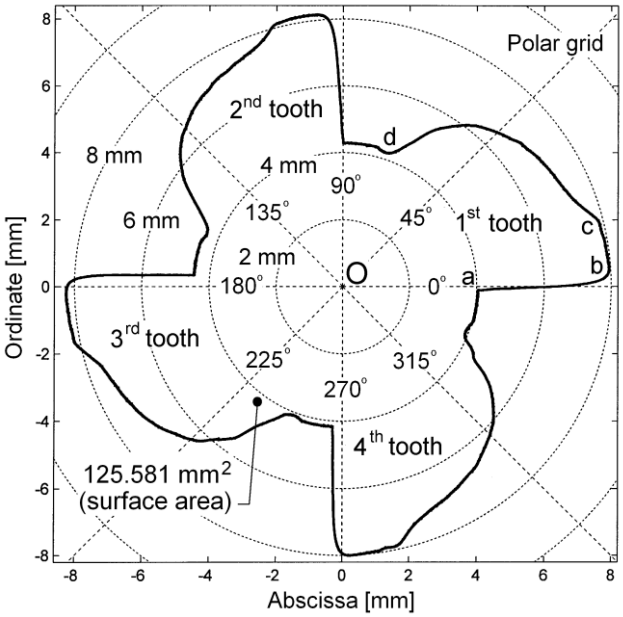

Fig. 9 – The experimental 2D cross section profile of the four flute end mill (with R_i = 4.25 mm).

A quick way to detect if the tool is damaged is to compare this type of profile with the profile of a new tool (used as a pattern), or with a profile obtained by numerical simulation for a perfect tool (without run-out, without sharp edges rounding) as Fig. 8 indicates.

A better manner to use this experimental approach is of course the representation of the 2D cross section profile using the known value of radius for inscribed circle (here R_i = 4.25 mm), as Fig. 9 indicates. In order to have as reference the abscissa and ordinate axis the profile has been rotated until the edges are placed approximately on these axes. It is obvious on Fig. 9 that despite the run-out effect, the teeth are not symmetrical. Of course this is not a critical item in milling tool manufacturing and perhaps there is a positive effect on cutting process (in diminishing the phenomenon of chatter).

A simple way to detect if the tool is damaged is to calculate the surface area of the region bordered by this 2D profile. A first indicator of damaging is the diminishing of this surface area (compared with the area of a perfect tool). A simple way to calculate this surface area is to use elementary triangles. The 2D profile is defined with *m* points (here *m* = 45300) and *m* lines segments between each two neighboring points (as end points). There are *m* elementary triangles defined by each two neighboring points together with the center O (placed in the origin of Cartesian coordinate system). Let P_i and P_{i+1} be two arbitrary neighboring points together with the origin point O as defining an elementary triangle. The sum of the areas of all these *m* elementary triangles (http://www.mathopenref.com/coordtrianglearea.html) defines with a good approximation the surface area A_{csp} of the zone bordered by this 2D cross section profile, written as:

$$A_{csp} = \sum_{i=1}^{m-1} \frac{P_i^x \cdot (P_{i+1}^y - O^y) + P_{i+1}^x \cdot (O^y - P_i^y) + O^x \cdot (P_i^y - P_{i+1}^y)}{2} \tag{7}$$

Here *x* and *y* are conventionally written as exponents to indicate the abscissa and the ordinate values of each point. Because $O^x = 0$ and $O^y = 0$ the Eq. (7) can be rewritten in a simpler form:

$$A_{csp} = \sum_{i=1}^{m-1} \frac{P_i^x \cdot P_{i+1}^y - P_{i+1}^x \cdot P_i^y}{2} \tag{8}$$

The surface area calculated using the above equation is: A_{csp}=125.581 mm^2 (a value already written on Fig. 9).

A frequent deficiency of milling tools is related with the presence of built-up edges. In order to simulate this presence, a small piece of beeswax was placed on the rake face of the first tooth of the four flute end mill.

The detection of 2D cross section profile was done again in these conditions. Fig. 10 present booth profiles: the previous one (already depicted in Fig. 9) and the new one (with a simulated built-up edge, which correspond to the area filled with black color).

We should mention here an insufficiency of this detection technique: sometimes (also in this case) the profiles don't have the same angular origin (introduced in Fig. 1) so the second profile is placed in a different angular position. In order to obtain the description from Fig. 10, the new profile was manually rotated (by data processing) until a totally fit was revealed (except the built-up edge area). In order to solve this problem, a computer assisted technique of 2D profiles fitting will be developed in the near future.

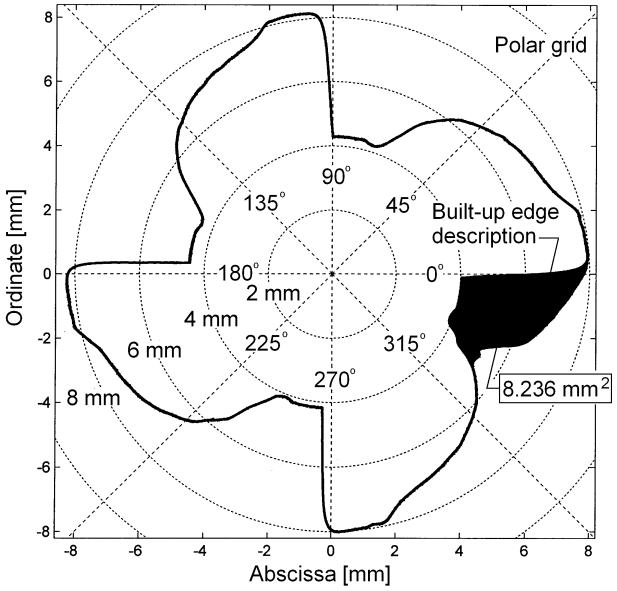

Fig. 10 – The detection and the description of a simulated built-up edge on the milling tool depicted in Fig. 9.

The surface area A_{csp} of the new profile was calculated in the same way (A_{csp} = 133.816 mm^2) so the built-up edge is described by a surface area of 133.816-125.581 = 8.236 mm^2. It is confirmed that the placement the size and the dimension of the built-up edge (or other deficiencies, as tooth breakage or a major wear) can be accurately determined.

It is obviously that all the considerations done before are available for any other rotating object. As example, Fig. 11 presents a result related with the description of a profile on a workpiece (with a hexagonal cross section). It describes the unadulterated profile (A_{csp} = 2087.56 mm^2) and the profile with a permanent magnet attached (A_{csp} = 2159.60 mm^2). The influence of the magnet

on the profile (an increasing of 72.04 mm^2 on surface) corresponds to the area filled with black color.

The hexagonal profile is relatively well mirrored (except -as expected- the rounded corners). A computer aided study related to profile geometry accuracy can be easy achieved (as a future activity). On the contrary, the profile of the magnet (the black filled area on Fig. 11, which should appear almost as rectangular) is not well described. The main reason for this negative aspect is that the magnet (a rare earth magnet, NdFeB) is covered with a strong reflective layer (for protection). Because the optical working principle of the sensor, the reflectance of this layer strongly distorts the result of magnet shape monitoring. This distortion is also related to the rotation direction (clockwise direction on Figs. 7 ÷11).

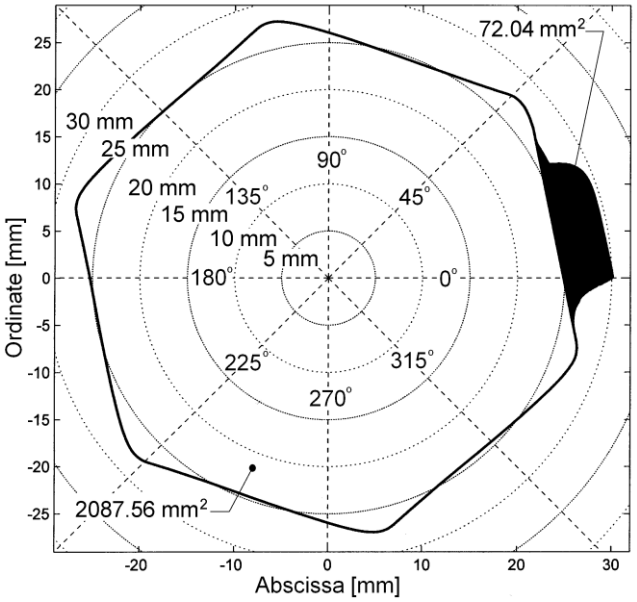

Fig. 11 – The detection and the description of a hexagonal 2D cross section profile (with and without altered shape) on a rotating workpiece (1043.35 rpm rotational speed, with T = 57.507 ms, m = 11502, p = 8, Δt = 5 μs, $\Delta\varphi$ = 546.3 μrad, R_i = 24.7 mm).

It is easy to imagine now a 3D description technique of a rotating object. Let Oz be the third axis (z-axis) of the Cartesian coordinate system (placed on the rotating axis of the object). Let Δz be an increment of displacement on z-axis. If the 2D cross section profiles are acquired in different positions on z axis (with Δz distance between) then is easy to find out a 3D graphic form of description for the rotating object. Also is possible (and more efficient) to describe the 3D shape of the object with a continuous rotation (with known angular speed) and continuous displacement on z-axis (with known

linear speed). In these conditions the experiment will produce a continuous 3D helical curve placed on the rotating object.

In both situations the 2D profile in different axial positions or the 3D continuous curve can be automatically converted in a volume. The analysis of this volume can provide in a simple manner many useful information related to the condition of the rotating body being analyzed.

This computer assisted monitoring technique can be easy implemented in different industrial applications and especially as an additional surveillance facility system for milling (or drilling) tools condition on CNC milling machines.

4. Conclusions

The computer assisted technique described in this paper proposes the computer aided 2D cross section profile detection of rotating objects. A theoretical and an experimental approach is presented (the equipment, the experimental setup, the data signal processing procedures and experimental results) in order to prove the availability of this technique.

Two common used rotating objects with relative complicated cross section profiles in machining industry were analysed in experimental terms: a milling tool (a four flute end mill) and a workpiece (with hexagonal cross section).

Despite some deficiencies (with known causes) the accuracy of the experimentally determined profiles is high enough in order to detect and to characterize the major parts of possible deviations from the expected shape and dimensions of these profiles. If we consider the milling tools as rotating objects, this technique is able to detect the braking, cracking, built-up edges, a deep wear of cutting parts, etc.

A simple way for automatic detection of the 3D shape, size and dimensions of rotating objects is also preliminary described (as a challenge for the future activity). The 3D profiling will offer a more complete characterization of rotating object.

Some other resources of experimental research will be also exploited: the increasing of measurement range and sampling rate of the sensor, the increasing the accuracy of the profiles by calibration, detection of hidden areas, etc. For the time being the optical sensor has the incident and reflected laser beams (30 degrees between) placed in the same plane with the 2D profile. It is expected that if these plane are perpendicular the profile will be defined more accurately.

Acknowledgements. I have to mention here the generosity of Mr. Eugen CARATA (full professor, PhD) who provided me the optical sensor together with some precious experimental advices. I should mention also that the main ideas of this study

were independently formulated as a consequence of theoretical and experimental support given to Mr. Mihai BOCA (lecturer, PhD) during his PhD thesis achievement. This was a pleasant and stimulating activity for me.

REFERENCES

Abu-Nabah B.A., ElSoussi A.O., ElRahman A., AlAlami K., *Simple Laser Vision Sensor Calibration for Surface Profiling Applications*, Optics and Lasers in Engineering, **84**, 51-61 (2016).

Bi Z.M., Wang L., *Advances in 3D Data Acquisition and Processing for Industrial Applications*, Robotics and Computer-Integrated Manufacturing **26**, 403-413 (2010).

Dhanasekar B., Ramamoorthy B., *Restoration of Blurred Images for Surface Roughness Evaluation Using Machine Vision*, Tribology International **43**, 268-276 (2010).

Ding Y., Zhang X., Kovacevic R., *A Laser-Based Machine Vision Measurement System for Laser Forming*, Measurement, **82**, 345-354 (2016).

Fernández-Roblesa L., Azzopardib G,, Alegre E., Petkov N., *Machine-Vision-Based Identification of Broken Inserts in Edge Profile Milling Heads*, Robotics and Computer–Integrated Manufacturing, **44**, 276-283 (2017).

Ghosh N., Ravi Y.B., Patra A., Mukhopadhyay S., Paul S., Mohanty A.R., Chattopadhyay A.B., *Estimation of Tool Wear During CNC Milling Using Neural Network-Based Sensor Fusion*, Mechanical Systems and Signal Processing, **21**, 466-479 (2007).

Kapłonek W., Nadolny K., *Laser Methods Based on an Analysis of Scattered Light for Automated, In-Process Inspection of Machined Surfaces: A Review*, Optik, **126**, 2764-2770 (2015).

Loizou J., Tian W., Robertson J., Camelio J., *Automated Wear Characterization for Broaching Tools Based on Machine Vision Systems*, Precision Engineering, **44**, 236-244 (2015).

Mendikute A., Zatarain M., *Automated Raw Part Alignment by a Novel Machine Vision Approach*, Procedia Engineering, **63**, 812-820 (2013).

Quinsat Y., Tournier C., *In Situ Non-Contact Measurements of Surface Roughness*, Precision Engineering, **36**, 97-103 (2012).

Svalina I., Simunovi G., Sari T., Lujic R., *Evolutionary Neuro-Fuzzy System for Surface Roughness Evaluation*, Applied Soft Computing **52**, 593-604 (2017).

Szydłowski M., Powałka B., Matuszak M., Kochmanski P., *Machine Vision Micro-Milling Tool Wear Inspection by Image Reconstruction and Light Reflectance*, Precision Engineering, **44**, 236-244 (2014).

Xing Z., Chen Y, Wang X., Qin Y., Chen S., *Online Detection System for Wheel-Set Size of Rail Vehicle Based on 2D Laser Displacement Sensors*, Optik **127**, 1695-1702 (2016).

Zatarain M., Mendikute A., Inziarte I., *Raw Part Characterization and Automated Alignment by Means of a Photogrammetric Approach*, CIRP Annals - Manufacturing Technology, **61**, *1*, 383-386 (2012).

** http://www.img.ufl.edu/wiki/images/ILD_2000_Datasheet.pdf (accessed on 6.01.2017).

[*] https://www.picotech.com/download/datasheets/picoscope-4000-series-data-sheet.pdf (accessed on 6.01.2017).

[*] http://www.mathopenref.com/coordtrianglearea.html (accessed on 6.01.2017).

DEDUCEREA PROFILULUI TRANSVERSAL 2D PENTRU OBIECTE CU MIŞCARE DE ROTAŢIE CU UTILIZAREA UNUI SISTEM DE MĂSURĂ OPTIC, FĂRĂ CONTACT

(Rezumat)

Lucrarea prezintă unele rezultate ale cercetării legate de studiul experimental asistat de calculator a formei secţiunilor transversale ale obiectelor cu mişcare de rotaţie (în particular o freză cilindro-frontală cu diametrul de 16 mm). Ca senzor este utilizat un sistem optic/laser de măsurare a deplasării relative, plasat în proximitatea sculei.

Semnalul furnizat de senzor (corelat cu caracteristicile mişcării de rotaţie) este utilizat pentru a produce reprezentarea grafică plană, bidimensională, a secţiunii transversale a obiectului. Experimentele au demonstrat că există suficiente elemente de similitudine a acestei reprezentări cu profilul real, care să asigure un grad ridicat de încredere în calitatea rezultatelor. Astfel forma, dimensiunile şi integritatea unei scule pot fi evaluate direct pe maşina-unealtă, pentru a asigura creşterea siguranţei în exploatare (în special pentru prevenirea lucrului cu o sculă defectă sau neadecvată). Există toate premizele dezvoltării acestei tehnici la determinarea descrierii tridimensionale a obiectelor rotative.